Volume 2
Number 3
May 2025
Pages 429-658

RSC Pharmaceutics

rsc.li/RSCPharma

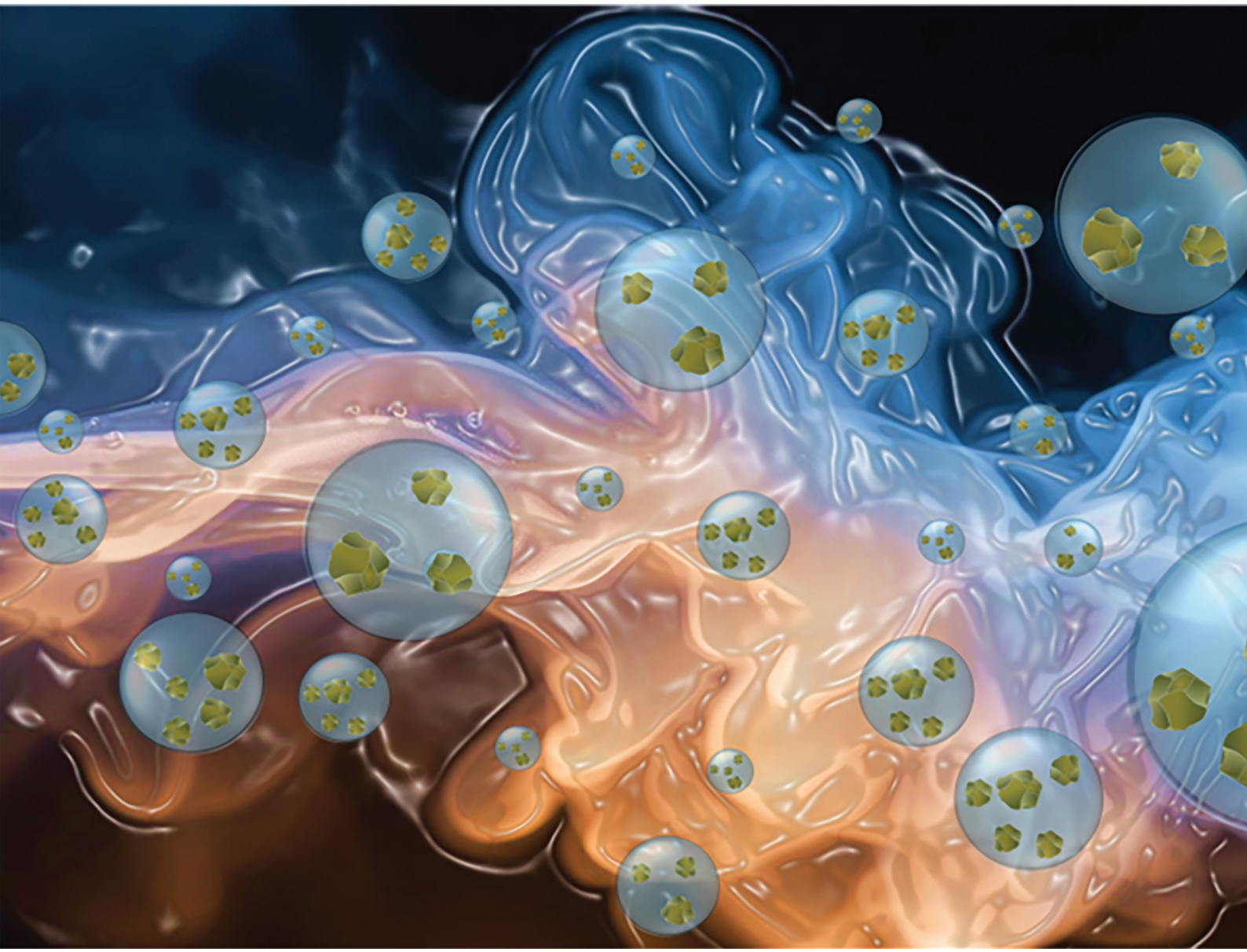

eISSN 2976-8713

ROYAL SOCIETY OF CHEMISTRY

COMMUNICATION

Steve P. Rannard *et al.*

Development of solid drug nanoparticle dispersions for pulmonary delivery of niclosamide and nitazoxanide *via* vibrating mesh nebulisation

RSC Pharmaceutics

ROYAL SOCIETY OF CHEMISTRY

COMMUNICATION

View Article Online
View Journal | View Issue

Check for updates

Cite this: *RSC Pharm.*, 2025, **2**, 517

Received 10th January 2025,
Accepted 28th March 2025

DOI: 10.1039/d5pm00006h

rsc.li/RSCPharma

Development of solid drug nanoparticle dispersions for pulmonary delivery of niclosamide and nitazoxanide *via* vibrating mesh nebulisation†

Catherine Unsworth,[a,b] Andrew B. Dwyer,[a,b] Alison C. Savage,[a,b] James J. Hobson,[a,b] Jonathan Massam,[a,b] Tom O. McDonald,‡[a] Paul Curley,[b,c] Andrew Owen,[b,c] Andrew O'Sullivan,[d] Ronan MacLoughlin[d] and Steve P. Rannard*[a,b]

The optimum delivery of very poorly soluble drug compounds is challenging, especially if targeting of disease sites is required. Delivery to the lung is hampered by a range of physiological issues, and inhalation may be the most appropriate route. When breathing is compromised by infection or poor lung capacity, nebulisation may enable therapeutics to be carried deep into the respiratory tract. Here we report the development of nebulised aqueous formulations of two highly water-insoluble drugs with demonstrated anti-SARS-CoV-2 activity and evaluate their pulmonary delivery using *in vitro* models that include the breathing patterns of children and COVID-19 infected adults.

Open Access Article. Published on 01 April 2025. Downloaded on 1/18/2026 4:55:59 AM.
This article is licensed under a Creative Commons Attribution 3.0 Unported Licence.

Introduction

Chronic pulmonary and respiratory conditions are included within the list of major non-communicable disease areas facing global healthcare systems, with increasing prevalence due to a range of causes including climate change, airborne pollution, smoking of tobacco products, and vaping.[1,2] The emergence of new respiratory pathogens, such as the recent coronaviruses Middle East respiratory syndrome (MERS-CoV), severe acute respiratory syndrome coronavirus (SARS-CoV) and severe acute respiratory syndrome coronavirus 2 (SARS-CoV-2), have also demonstrated the ongoing threat of acute respiratory infection to human life.[3]

The direct delivery of therapeutics to the respiratory tract and deeper lung regions poses several challenges. Solid particulate powder and aerosol delivery is hampered by the highly bifurcating architecture of the lungs, the progressive narrowing of airways and the different angles within the branched structure. This encourages impact of airborne particulates onto lung surfaces. Additionally, the high humidity and the presence of the mucociliary escalator, as the primary route for clearance, limit drug residence times and, therefore, impact efficacy.[4,5]

Many dry inhaled medicines rely on engineered and porous, low-density carrier particles to augment the delivery of encapsulated drug compounds. Nebulised medicines may utilise aqueous drug solutions or suspensions.[6] Penetration into the alveolar regions is of particular interest and nanoparticle (or sub-micron) drug formulations have received significant interest.[7] Despite the relatively low availability of bulk water to aid the solubility of poorly water-soluble compounds within the lung, the low particle size and high surface area of nanoparticles within the dosed drug mass is expected to aid penetration, deposition and dissolution kinetics.[8] Development strategies have utilised nanocarriers generated from polymers, such as poly(lactic-*co*-glycolic acid) (PLGA), or liposomal formulations.[9]

Solid drug nanoparticles (SDNs) are sub-micron particles that are formed entirely of drug compound with aggregation avoided by absorbed polymer and/or surfactant stabilisers.[10] There are several techniques for the production of SDNs from poorly water-soluble drug compounds including nanomilling,[11] high pressure homogenisation,[12] emulsion freeze drying/spray drying,[13–19] and nanoprecipitation techniques.[20–22]

Two drug compounds of considerable pulmonary potential are niclosamide (NCL) and nitazoxanide (NTZ). NCL is a salicylanilide anthelmintic agent, listed by the World Health

[a]*Department of Chemistry, University of Liverpool, Crown Street, Liverpool, L69 7ZD, UK. E-mail: srannard@liverpool.ac.uk*
[b]*Centre of Excellence in Long-acting Therapeutics (CELT), University of Liverpool, Liverpool, L7 3NY, UK*
[c]*Department of Pharmacology and Therapeutics, University of Liverpool, Sherrington Building, Ashton Street, Liverpool L69 3GE, UK*
[d]*Research and Development, Science and Emerging Technologies, Aerogen Limited, Galway Business Park, Dangan, Galway, H91HE94, Ireland*
†Electronic supplementary information (ESI) available. See DOI: https://doi.org/10.1039/d5pm00006h
‡Current address: Department of Materials, The University of Manchester, Oxford Road, Manchester, M13 9PL, UK and Henry Royce Institute, The University of Manchester, Oxford Road, Manchester, M13 9PL, UK.

© 2025 The Author(s). Published by the Royal Society of Chemistry

Open Access Article. Published on 01 April 2025. Downloaded on 1/18/2026 4:55:59 AM. This article is licensed under a Creative Commons Attribution 3.0 Unported Licence.

Organisation (WHO) as an Essential Medicine,[23] and is the subject of numerous reports showing efficacy against diseases including viral infections,[24,25] several forms of cancer,[26–29] and Parkinson's disease.[30] Importantly, it also displays bronchodilation properties, providing additional potential in the treatment of respiratory diseases including asthma, cystic fibrosis, and chronic obstructive pulmonary disease.[31] NTZ is a nitrothiazole benzamide broad spectrum antiparasitic and antibacterial agent with reported additional broad spectrum antiviral activity.[32] Both drugs are highly insoluble in water (NCL $\approx$ 6 μg mL^{-1} and NTZ = 7.66 μg mL^{-1}),[33–36] and have shown efficacy against SARS-CoV-2.[37–40]

NCL and NTZ are Biopharmaceutics Classification System class II molecules, resulting in very low oral bioavailability and, therefore, have limited systemic drug concentrations after oral administration.[41,42] Accumulation of either drug at a primary pulmonary site of infection is unlikely with conventional oral medicines; however, both drugs are good candidates for pulmonary delivery as aqueous SDN dispersions. Aerosol delivery is classed as a non-invasive administration route with the considerable benefit of self-administration if required, reducing clinic and contact time for both patients and heath care professionals. Delivery may be targeted directly to the lungs, improving efficacy and clinical outcomes.[43,44]

SDNs of NCL have been reported through high-pressure homogenisation and recovery *via* spray drying, with studies as an inhalable medicine candidate after redispersion in saline solution.[45] A high level of mannitol (up to 10× the mass of NCL) was required in these studies to stabilise the particles during drying, considerably exceeding amounts in currently approved products. NCL/human lysozyme nanoparticles suitable for delivery *via* a dry powder inhaler or using a nebuliser/nasal spray after dispersion in a suitable medium, have also been reported.[46] Within these formulations the maximum possible NCL loading was <1% w/w within the dry mass, significantly reducing the deliverable dose of NCL with respect to total mass inhaled. Inhalable NTZ formulations have also been reported using PLGA nanocarrier encapsulation.[47]

We recently demonstrated the scalable nanoprecipitation of NCL and maintenance of *in vivo* long-acting systemic drug exposure after intramuscular administration of an aqueous NCL SDN dispersion.[48] Here we evaluate nanoprecipitation as a route to generate SDN formulations of NCL and NTZ for inhaled delivery using vibrating mesh nebulisers (VMNs), with studies to model lung delivery for healthy and compromised breathing patterns.

Results and discussion

Synthesis and characterisation of solid drug nanoparticles of niclosamide and nitazoxanide

The synthesis and characterisation of NCL SDNs has been previously reported *via* flash nanoprecipitation methodology and was utilised without modification in this study.[48] In summary, an NCL solution in 80/20 (v/v) acetone/ethanol at 60 °C (Fig. 1A) was rapidly added to an aqueous solution containing hydroxypropyl methyl cellulose (HMPC) and sucrose with fast stirring, followed by sonication (Fig. 1B). The resulting suspension was spray dried to remove the aqueous and organic solvents and produce a fine powder containing nanoparticles of NCL (Fig. 1C) that could be readily redispersed into water.

Establishing the ideal nanoprecipitation conditions for NTZ required the formation of a drug solution in a water-miscible solvent environment. Dimethyl sulphoxide (DMSO) was found to generate a 200 mg mL^{-1} solution at ambient temperature and used to screen a number of combinations of possible excipient stabilisers under flash nanoprecipitation conditions. The selected stabiliser options were poly(vinyl alcohol) (PVA), Pluronic F127® (F127), Pluronic F68® (F68), HPMC, hydroxypropyl cellulose (HPC), Tween® 20, Tween® 80 and sodium dodecyl sulfate (SDS). Each excipient was selected based on its use within the NCL SDN formulations and a thorough study of materials utilised in FDA approved inhalable medicines (FDA Centre for Drug Evaluation and Research (CDER) list of Inactive Ingredients) or reviewed in literature reports of pulmonary delivery.[49–52] Following the procedure for the synthesis of NCL SDNs, the NTZ DMSO solutions were added to aqueous solutions of binary combinations of excipients. A matrix of fifteen nanoprecipitations were conducted, utilising either Tween® 20, Tween® 80 or SDS as the secondary (2°) excipient and combining with each of the remaining materials as a primary (1°) excipient (namely PVA, F127, HPMC, F68 or HPC) to form a library of 70/20/10 wt% combination of NTZ/1°/2° excipient formulations. Within this screen, the DMSO content within the final aqueous flash nanoprecipitation medium was 17.5% v/v leading to a solids content of 5% w/v. After spray drying, followed by freeze drying to ensure complete removal of DMSO, the samples were redispersed into saline solution (0.9% w/v) at an NTZ concentration of 1 mg mL^{-1} for dynamic light scattering (DLS) studies using a Malvern Panalytical ZetaSizer Ultra. For application as a dispersion within the Aerogen Solo VMN (Fig. 1D), *z*-average particle diameters (D_z) of <1 μm were targeted. Unfortunately, the fifteen formulations generated poor quality dispersions or poor distributions D_z = 1.3–2.0 μm (ESI Table S1†). Combinations of F127 and Tween® 20, however, subjectively showed the highest potential within this screen.

The precipitation conditions were modified to reduce the DMSO content in the final aqueous phase after flash nanoprecipitation to 10% v/v, thereby reducing the amount of good solvent in the final precipitation mixture. A 50 wt% content of NTZ was targeted in the final formulation (relative to excipients) and the remaining 50 wt% of the formulation relating to 1° and 2° excipients was altered systematically from 40/10, 30/20, 20/30, 10/40 respectively, whilst maintaining a 5% w/v solids content overall. None of these variations led to stable particle dispersions after redispersion into saline and the recovered samples were less solid, leading to handling problems.

Pulmonary formulations have utilised lactose as a carrier material for many years,[53] therefore lactose was added into the

© 2025 The Author(s). Published by the Royal Society of Chemistry

Open Access Article. Published on 01 April 2025. Downloaded on 1/18/2026 4:55:59 AM.
This article is licensed under a Creative Commons Attribution 3.0 Unported Licence.

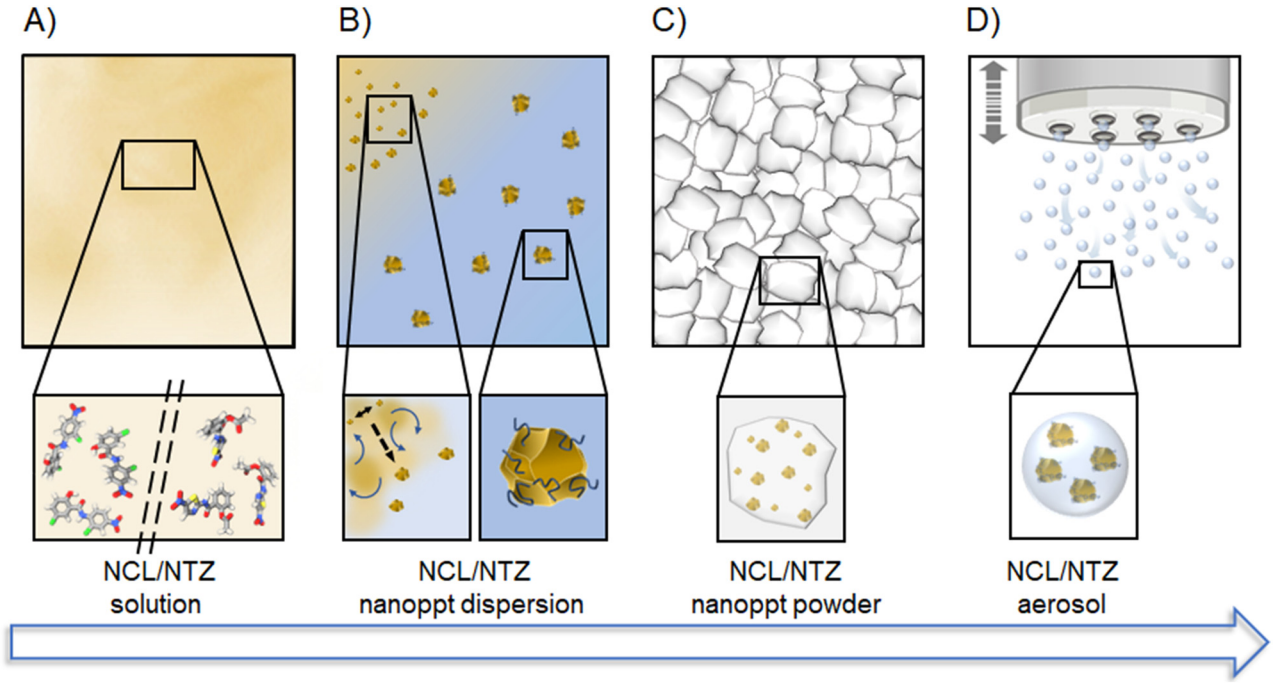

Fig. 1 Schematic representation of the formation of nebulised SDN dispersions. (A) Formation of a solution of niclosamide (NCL) or nitazoxanide (NTZ) in a water-miscible good solvent. (B) Addition of the solution to water (acting as a poor solvent) containing stabilisers – rapid diffusion of the good solvent leads to supersaturation and particle formation. (C) Spray drying of the aqueous/solvent dispersion to form a powdered composite product comprising a matrix of water-soluble stabilisers and solid drug nanoparticles (SDNs). (D) Redispersion of the spray dried product into saline and vibrating mesh nebulisation to form aerosol droplets containing drug particles.

aqueous precipitant medium as a tertiary (3°) excipient. Nanoprecipitation formulation screening was restricted to F127 and Tween® 20, with initial results having shown this excipient combination to offer the greatest potential. Studies continued to utilise a 50 wt% NTZ content (relative to excipients) whilst varying the 1°/2°/3° excipient ratio systematically from 30/10/10 to 10/20/20, with some samples having no F127 or Tween® 20 to explore the importance of a ternary stabiliser combination. A considerable improvement in solid nature of the samples was immediately seen. The polydispersity (PdI) of the redispersed samples also improved with a general decrease in D_z values, with the best formulation being: $NTZ_{50}/F127_{20}/lactose_{30}$, D_z = 860 nm and PdI = 0.282 (ESI Table S2†).

Further iteration of the F127/lactose ratio, whilst maintaining a 50 wt% NTZ concentration in the solid product, showed no significant improvement and increasing the NTZ content to 60 wt% led to a general increase in D_z and PdI values to D_z > 1 μm and PdI > 0.450, Table 1. Interestingly, the substitution of lactose for the alternative disaccharide, sucrose, led to a considerable decrease in D_z values when targeting 60 wt% NTZ in the final solid formulation, Table 1. The beneficial introduction of sucrose mirrored our previous NCL formulation[48] and offered a simplified binary formulation for the NTZ SDN nanoprecipitation.

The lead formulation, showing good reproducibility and relatively low D_z values, Fig. 2B, was selected as $NTZ_{60}/F127_{20}/Sucrose_{20}$. This was reproduced at a total formulation mass of 7.5 g with excellent scalability when compared with the small-scale sample production. The solid product was a free-flowing powder with excellent redispersion into saline with hand shaking.

Table 1 Composition of developmental nitazoxanide (NTZ) formulations and corresponding physical characterisation data, measured using Dynamic Light Scattering (DLS). Solid drug nanoparticle powder dispersed at 1 mg mL^{-1} in 0.9% w/v saline

Formulation composition (wt%)				DLS analysis	
NTZ	F127	Lactose	Sucrose	D_z (nm)	PdI
50	30	20	—	900	0.437
	25	25	—	850	0.372
	20	30	—	860	0.282
60	30	10	—	850	0.377
	25	15	—	1080	0.471
	20	20	—	1030	0.519
	15	25	—	1090	0.520
60	30	—	10	700	0.390
	20	—	20	680	0.388
	10	—	30	820	0.353
60[a]	20[a]	—	20[a]	700	0.197

[a] Scale up sample containing 4.5 g NTZ.

Analysis of the scaled sample using reverse-phase high performance liquid chromatography (RP-HPLC) confirmed the expected loading of NTZ (wt% relative to excipients) within the

© 2025 The Author(s). Published by the Royal Society of Chemistry

Open Access Article. Published on 01 April 2025. Downloaded on 1/18/2026 4:55:59 AM.
This article is licensed under a Creative Commons Attribution 3.0 Unported Licence.

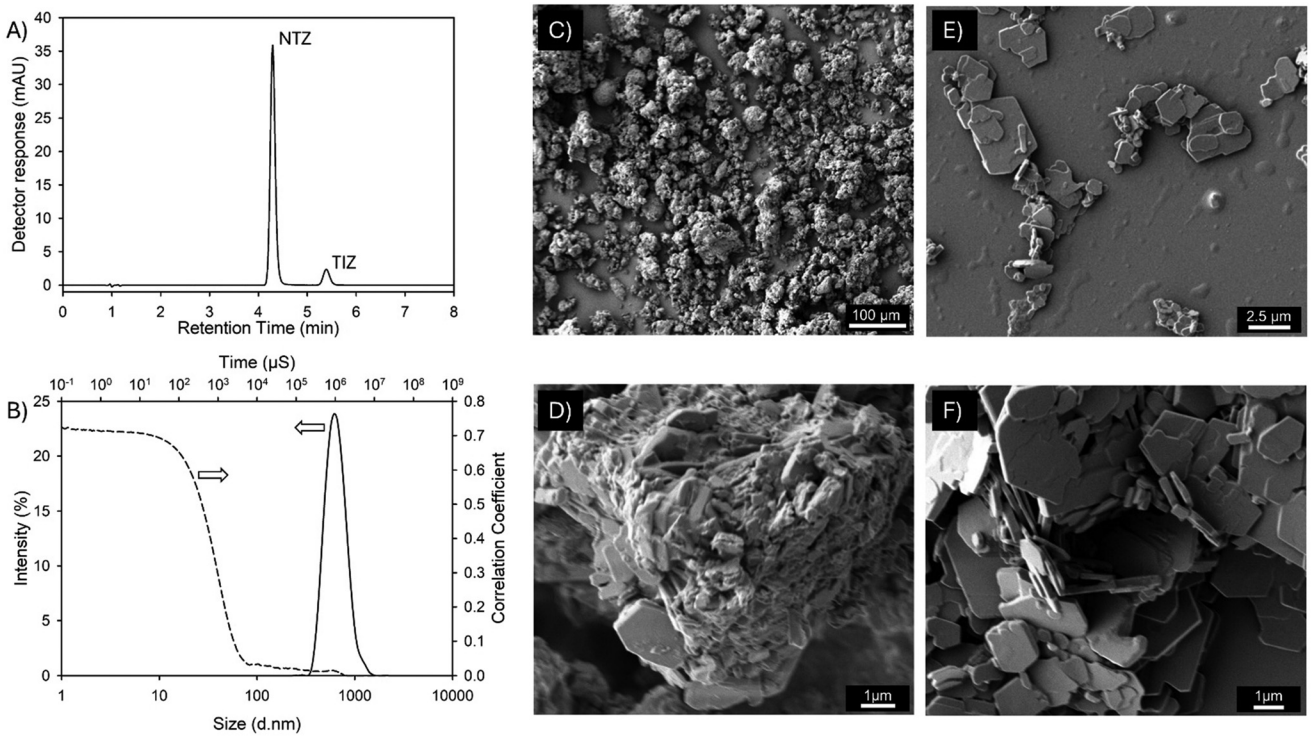

Fig. 2 Characterisation of lead formulation containing 60 wt% nitazoxanide (NTZ), 20 wt% pluronic F127, 20 wt% sucrose. (A) HPLC analysis showing both NTZ and tizoxanide (TIZ; active metabolite) peaks, (B) particle size and distribution analysed by dynamic light scattering at 1 mg mL^{-1} in 0.9% w/v saline, (C) and (D) scanning electron micrograph (SEM) analysis of spray dried solid drug nanoparticle powder, (E) and (F) SEM analysis of NTZ formulation dispersed at 1 mg mL^{-1} in water.

spray dried powders (ESI Fig. S1 and 3†) and indicated the presence of two peaks that were identified as NTZ and tizoxanide (TIZ), the active metabolite of NTZ formed by deacetylation, presumably during the preparation or analysis of the SDN samples, Fig. 2A. At this investigation stage, the presence of the active metabolite of NTZ is not considered a major concern.

The spray dried powders containing NCL SDNs, and dried SDN dispersions have been previously studied by scanning electron microscopy (SEM).[48] A similar study was conducted to assess the morphology of the spray dried powders containing NTZ SDNs and the dried dispersions, Fig. 2C–F. Particles within spray dried powders have been reported with many process-dependent structures,[54] and the nature of feedstocks may alter the characteristics of powders formed from dispersions rather than solutions.[55] NTZ SDN powders showed complex structures that appeared to differ considerably from a conventional dried droplet, typically seen when spray drying solutions, Fig. 2C, and on closer examination it was apparent that the powder particles comprised large numbers of platelet structures that appeared bound together into bundles/aggregates, Fig. 2D. Dispersion of the powder into water and subsequent drying onto the SEM stub for analysis, confirmed a relatively broad distribution of thin NTZ platelet structures were present, Fig. 2E and F. This contrasted to SEM analysis of bulk powder (ESI Fig. S4†), indicating a more complicated mechanism during the addition of the NTZ solution to the aqueous poor solvent environment than would typically be expected from nanoprecipitation.

Many parameters are known to impact the formation of particles during precipitation processes such as those employed here. For example, the supersaturation stages experienced by the drug molecules after the good solvent solution is added to the aqueous antisolvent mixture of stabilisers are modified by drug concentration, rate of addition, efficiency of mixing, temperature and the chemical nature of the dissolved drug molecule and the stabilisers present.[22,56]

Under these conditions, the formation of NTZ particles with a platelet morphology, consistent D_z and PdI values was extremely robust, and the formulation was utilised for nebulisation studies.

Nebulisation studies using aqueous dispersions of NCL and NTZ

The formation of stable dispersions of NCL and NTZ SDNs in saline solutions was important for the intended use of nebulisation using a VMN. Due to the isotonic nature of saline solutions, their use is particularly beneficial for preventing drying of the airways during pulmonary drug delivery.[57] More importantly, the electrolyte concentration has a significant impact on solution conductivity and can impede the piezo-electric actuation mechanism if too low.[58] Critically, the VMN process

© 2025 The Author(s). Published by the Royal Society of Chemistry

Open Access Article. Published on 01 April 2025. Downloaded on 1/18/2026 4:55:59 AM. This article is licensed under a Creative Commons Attribution 3.0 Unported Licence.

forms an aerosolised mist from the bulk liquid and the dispersed drug particles are expected to be dispersed within the aerosolised droplets, in a manner not dissimilar to the spray drying of a dispersion or suspension (Fig. 1D). VMN delivery of aerosolised drug has been shown to be more efficient than other means of pulmonary delivery such as pressurised metered-dose inhalers and jet nebulisers.[59,60]

Several studies have reported the nebulisation of nanoparticle dispersions generated from biodegradable polymers,[61] hydrogels,[62] and liposomes,[63] but there have been relatively few reports of the use of nanoprecipitated SDN dispersions within nebulised formulations. A similar study of nebulisation reported the use of rod-like NCL nanoparticle dispersions formed by up to 20 cycles of high-pressure homogenization in the presence of different stabilisers, after pre-milling.[45]

Initial nebulisation studies of the NCL and NTZ dispersions (1, 5 and 10 mg mL^{-1}), using an Aerogen Solo VMN, involved loading the suspensions into the medication cup at the upper part of the nebuliser, with collection of the resulting aerosol in 50 mL centrifuge tubes and samples taken for particle size analysis, Table 2.

Studies showed efficient nebulisation of SDNs dispersed at 1, 5, and 10 mg mL^{-1} for both NTZ and NCL. For NCL nebulisation rate decreased as dispersion concentration increased. For NTZ there was no clear trend observed for nebulisation rate as a function of dispersion concentration. For all samples, at all concentrations tested, measured D_z of the dispersed formulations decreased after nebulisation. This is potentially due to the breakdown of larger particles during vibration, and of preferential nebulisation of smaller particles with the distributions.

Table 2 Nebulisation output rate of niclosamide (NCL) and nitazoxanide (NTZ) formulations using Aerogen Solo vibrating mesh nebuliser at concentrations of 1, 5, and 10 mg mL^{-1} dispersed in 0.9% w/v saline. Output rate was determined as mass of dispersion recovered after nebulisation. Dynamic light scattering analysis was performed on pre-nebulised dispersions and dispersions recovered post nebulisation, diluted to 1 mg mL^{-1} in 0.9% w/v saline

		Before nebulisation		After nebulisation	
API concentration (mg mL^{-1})	Output rate (g min^{-1})	D_z (nm)	PdI	D_z (nm)	PdI
NTZ					
1	0.291	1329	0.485	717	0.347
5	0.236	1447	0.536	606	0.237
10	0.267	1273	0.557	663	0.388
NCL					
1	0.326	719	0.272	589	0.226
5	0.269	823	0.305	542	0.216
10	0.170	698	0.268	547	0.245

Characterisation of the behaviour of nebulised aqueous NCL and NTZ SDN dispersions

The properties of NTZ and NCL dispersions were measured for inhalation applications by two orthogonal methods; laser diffraction (Table 3) and cascade impaction[64] (Next Generation Impactor (NGI); Fig. 3; Table 4), in accordance with international regulatory submission standards.[65] For clarity, the aerosol droplets are themselves liquid dispersions containing the SDNs of NTZ or NCL.

The NGI was not developed to act as an *in vitro* lung model and the collection stages do not represent any specific lung sites, however, a standardised section is present that assesses unwanted throat deposition and allows statements about expected penetration into the human lung to be made.[64] Aerosol formulations, with a droplet size distribution is introduced to the impactor through an induction port and at a constant flow (Fig. 3A). The NGI comprises seven stages, each with an impaction plate containing increasing numbers of holes with decreasing diameters (Fig. 3B). The aerosol flows through the stages consecutively, with each stage designed to remove a droplet fraction within a narrow diameter window through direct impaction on the surface of a removable collection cup (Fig. 3B). The remaining distribution passes through to the next impaction zone and another part of the distribution, of a smaller diameter, is similarly separated (Fig. 3C).

Laser diffraction[66] results provided the size distribution of aerosol droplets, along with the percentage of fine particle fraction (FPF) below 5 μm (Table 3). The FPF is the percentage of aerosol droplets containing SDNs that are small enough to enter the lungs and therefore deliver drug to the targeted site of action after nebulisation.[67] An Aerogen Solo VMN, was utilised in combination with an Aerogen Ultra and its mouthpiece to deliver each aerosol containing either 5 or 10 mg mL^{-1} of NTZ or NCL SDNs.

When increasing the drug concentration in the aerosolised SDN dispersions, a slight decrease in FPF was seen for both NTZ and NCL, however, the volume mean diameters at the 10, 50 and 90 percentiles were remarkably consistent between the aerosolised formulations containing the different drug sub-

Table 3 Results of laser diffraction analysis of nebulised lead formulations. The volume mean diameters, fine particle fraction (FPF), and flow rate of aerosol droplets were determined for niclosamide (NCL) and nitazoxanide (NTZ) formulations at 5 and 10 mg mL^{-1} in 0.9% w/v saline (Data shown as mean ± SD, n = 3)

API (mg mL^{-1})	D_{v10} (μm)	D_{v50} (μm)	D_{v90} (μm)	FPF% (<5 μm)	Flow rate (mL min^{-1})
NTZ					
5	1.22 (±0.07)	3.34 (±0.14)	7.41 (±0.28)	71.91 (±2.22)	0.37 (±0.02)
10	1.25 (±0.04)	3.59 (±0.02)	8.13 (±0.10)	67.58 (±0.33)	0.32 (±0.01)
NCL					
5	0.99 (±0.02)	3.43 (±0.07)	8.24 (±0.21)	68.27 (±1.13)	0.31 (±0.01)
10	1.04 (±0.01)	3.54 (±0.18)	8.40 (±0.43)	67.09 (±2.67)	0.23 (±0.03)

© 2025 The Author(s). Published by the Royal Society of Chemistry

Open Access Article. Published on 01 April 2025. Downloaded on 1/18/2026 4:55:59 AM.
This article is licensed under a Creative Commons Attribution 3.0 Unported Licence.

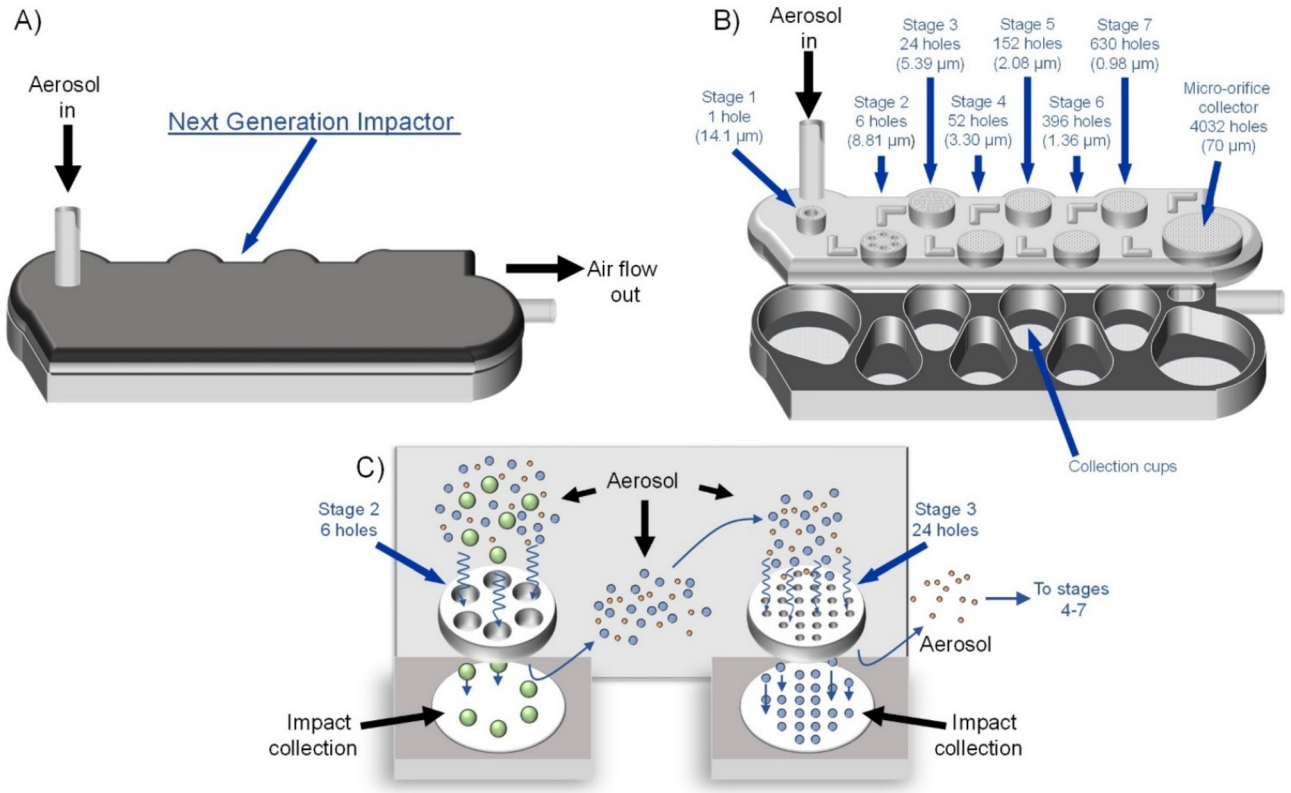

Fig. 3 Schematic of Next Generation Impactor (NGI) cascade impactor design. (A) The inlet and outlet points, direction of air flow, (B) the locations of the removable collection cups and cut-off sizes of the cup orifices, and (C) a demonstration of aerosolised droplet separation based on size are shown.

Table 4 Aerodynamic properties of aerosolised dispersions of niclosamide (NCL) and nitazoxanide (NTZ) lead candidate formulations including mass median aerodynamic diameter (MMAD), fine particle fractions (FPF), and flow rate of aerosol droplet at 5 and 10 mg mL^{-1} in 0.9% w/v saline, measured using the Next Generation Impactor (Data shown as mean ± SD, n = 3)

			FPF % (µm)			
NTZ (mg mL^{-1})	MMAD (µm)	GSD	≤5	2.3–5	≤2.3	Delivery Rate (mL min^{-1})
5	4.21 (±0.05)	1.54 (±0.02)	66.67 (±0.37)	64.02 (±0.18)	2.95 (±0.28)	0.35 (± 0.05)
10	4.08 (±0.16)	1.61 (±0.01)	67.75 (±2.95)	61.86 (±1.78)	5.90 (±1.17)	0.30 (± 0.01)
			FPF % (µm)			
NCL (mg mL^{-1})	MMAD (µm)	GSD	≤5	2–5	≤2	Delivery Rate (mL min^{-1})
5	3.98 (±0.22)	1.81 (±0.04)	65.77 (±4.29)	57.46 (±3.84)	8.31 (±0.75)	0.30 (±0.05)
10	3.62 (±0.21)	1.84 (±0.02)	70.36 (±3.14)	55.24 (±1.49)	15.24 (±2.99)	0.21 (±0.00)

stances. The FPF values of ≥67% are highly comparable with reports of aerosolised polymer nanoparticle dispersions containing a 1 : 20 w/w drug/polymer ratio,[68] although SDNs are able to inherently deliver more drug substance as they avoid encapsulation within polymeric nanocarriers.

Aerosol droplet size analysis measured by NGI showed values in agreement for FPF (<5 µm) values observed by laser diffraction (Table 4) and provided further insight into the size range of droplets within that fraction. The mass median aerodynamic diameter (MMAD) values for aerosols droplets containing SDNs from both NTZ and NCL were <4.5 µm with consistent dispersities, as shown by the geometric standard deviation (GSD) values. Both NTZ and NCL aerosolised dispersions displayed droplet sizes predominantly in the region of 2–5 µm, however the NCL dispersion had a higher fraction than the NCL of droplets smaller than 2.3 µm. Droplets of this size are known to penetrate deeper into the peripheral airways of the lungs.[69]

This was further evidenced when looking at the amount of NTZ or NCL deposited on the various collection plates of the NGI, with deposition on higher numbered plates indicative of increased aerodynamic efficiency of the particles (Fig. 4). Deposition into stages 4 and 5 approximates the central

© 2025 The Author(s). Published by the Royal Society of Chemistry

Open Access Article. Published on 01 April 2025. Downloaded on 1/18/2026 4:55:59 AM.
This article is licensed under a Creative Commons Attribution 3.0 Unported Licence.

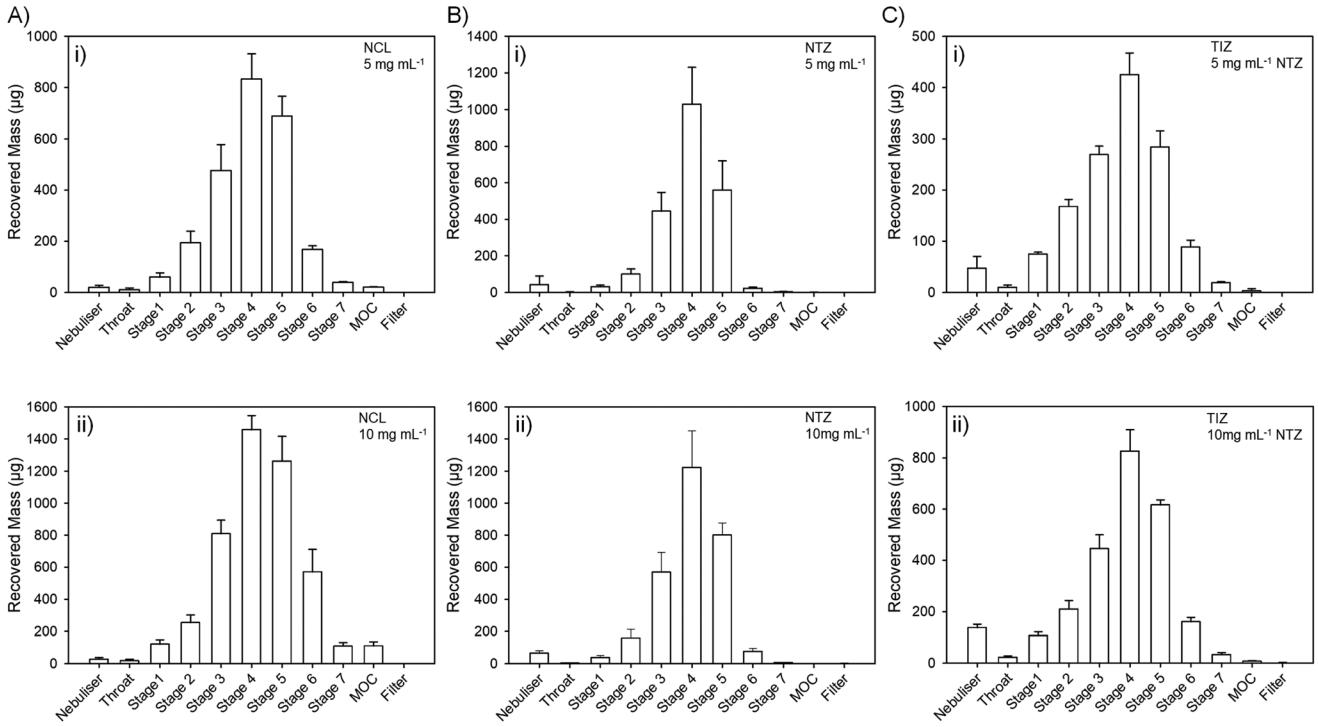

Fig. 4 Recovered mass of Niclosamide (NCL) (A), nitazoxanide (NTZ) (B) or its metabolite tizoxanide (TIZ) (C) detected at each stage of the cascade impactor, after nebulised dose of 5 mg mL^{-1} (i) or 10 mg mL^{-1} (ii). The direction of travel of the nebulised droplets goes from left to right, with deposition on higher numbered plates indicated a deeper penetration into the simulated breathing model, indicative of deeper penetration into the lungs. Samples were a quantified using RP-HPLC and data are shown as ±SD (n = 3). The Throat stage of the cascade impactor models human throat deposition and shows limited unwanted deposition in this region.

airways (trachea, primary and secondary bronchi), but, as mentioned previously, it is important to note that stages of the NGI do not directly relate to specific deposition sites within the lung.[64] For a total nebulised volume of 1 mL, the highest recovered masses were observed in plate 4 for both NTZ and NCL at both concentrations tested, with NCL having 0.832 mg and 1.457 mg for 5 and 10 mg mL-1 respectively, and with NTZ having equivalent recovered mases of 1.029 and 1.222 mg.

The deposition of either NCL (Fig. 4A) or NTZ (Fig. 4B) showed a similar profile within the NGI study, irrespective of the concentration of the nebulised SDN dispersion. TIZ deposition was also determined as relatively mild conditions can yield the active metabolite; it was clear that TIZ deposition largely mirrored that of the NTZ SDNs at both study concentrations (Fig. 4C).

Evaluation of nebulised aqueous NCL and NTZ SDN dispersions within simulated breathing models

NTZ and NCL have potential medicinal benefits within prophylaxis and treatment of active respiratory diseases. It is, therefore, important to evaluate the administration within an *in vitro* model of healthy and compromised patients, including adults and paediatric studies.

The nebulisable SDNs described above were studied using a breathing simulator able to model the pattern of adult and paediatric healthy breathing, and the altered breathing that is seen within adults experiencing the mild symptoms of SARS-CoV-2 infection (Fig. 5). NTZ and NCL were both independently nebulised at the two study concentrations of 5 and 10 mg mL^{-1} and the formulations were spiked with albuterol sulphate to act as an aerosol tracer within the simulator and

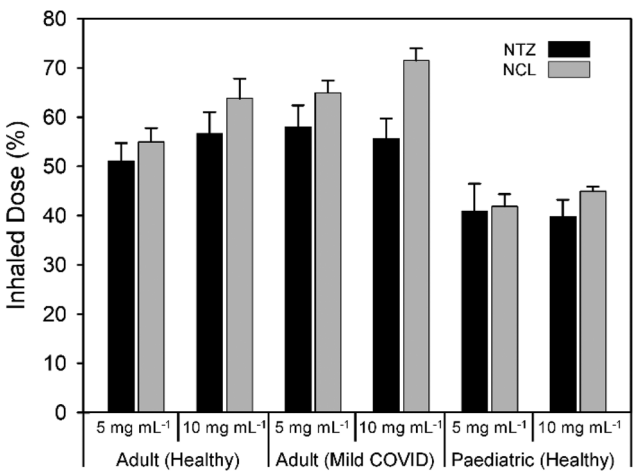

Fig. 5 Measurement of inhaled dose (%) of nitazoxanide (NTZ; black) and niclosamide (NCL; grey) formulation at 5 and 10 mg mL^{-1} concentration across three breathing patterns. Albuterol was used as a tracer to determine the deposition of the formulation. Dose was assessed at the exit of the mouthpiece, without use of a head model.

Open Access Article. Published on 01 April 2025. Downloaded on 1/18/2026 4:55:59 AM. This article is licensed under a Creative Commons Attribution 3.0 Unported Licence.

determine the inhaled NCL or NTZ dose within each breathing simulation;[43] this approach follows the international standard ISO27427:2023.[65]

A higher inhaled dose was observed with the NCL formulation at all administration concentrations and breathing models compared with the NTZ. This correlates with the NCL formulation exhibiting a slightly smaller MMAD and higher FPF below 2 μm, which allows for improved delivery of NCL.

Interestingly, the breathing pattern that models mild COVID-19 symptoms appears to aid the nebulised dose of the SDN dispersions. The higher breath rate (25 min^{-1} *vs.* 15 min^{-1} for healthy adults) and tidal volume (600 mL *vs.* 500 mL for healthy adults) may modify the flow of the nebulised dose to allow the improved inhalation. A symptom of COVID-19 is shortness of breath or dyspnea,[70] a state where breathing can become more rapid and deeper to compensate for lack of oxygen uptake. The influence of breathing patterns on the effectiveness of drug delivery by vibrating mesh nebuliser is well established in the literature.[71,72] For both the NTZ and NCL formulations, over 50% of the administered dose was inhaled for the adult breathing models, and over 39% was inhaled in the paediatric model, providing a clear indication that both the NTZ and NCL formulations are viable candidates for pulmonary drug delivery by nebulisation.

Conclusions

Solid drug nanoparticles are a nanocarrier free option for poorly water-soluble drug formulation. The aqueous dispersions appear to be nebulised without significant negative impact on the nebulisation process, delivered dose, movement of the aerosol, and deposition within areas deep within the lung. For very low water-solubility drugs like NTZ and NCL, this opens avenues of investigation for readily deployable inhalable therapeutics in the event of future emergencies and also the development of medicines to address unmet clinical needs within chronic disease conditions. The demonstration of future potential, that we present here, requires considerable preclinical pharmacokinetics, pharmacodynamics and safety evaluation, however, this proof-of-concept does generate considerable evidence to support further research.

Author contributions

CU, ABD, ACS, JJH, JM, PC and AOS carried out the investigation, analysis, methodology development and data visualisation. SR, TOM, AO and RM were responsible for conceptualisation of the research, project administration and supervision. SR and TOM were responsible for funding acquisition. SR and CU wrote the original draft of the manuscript and SR, CU, ABD, ACS, JJH, AO, AOS, TOM, and RM were responsible for review and editing.

Data availability

All data generated during this study supporting its findings are available within the manuscript and the ESI.† All data is available from the corresponding author upon reasonable request.

Conflicts of interest

CU, ABD, ACS, JJH, TOM, AO and SPR are coinventors of patents aiming to facilitate the rapid exploitation of the therapeutic options presented here. RM is a named inventor on multiple vibrating mesh nebuliser patents.

Acknowledgements

The authors wish to thank UK Research and Innovation for an Engineering and Physical Sciences Council (EPSRC) Impact Acceleration Award funding (EPSRC IAA: COVID-19) and funding *via* a Healthcare Impact Partnership Award (EP/R024804/1). This study was supported by funding from Unitaid project LONGEVITY (2020-38-LONGEVITY).

References

1 GBD Chronic Respiratory Disease Collaborators, *Lancet Respir. Med.*, 2020, **8**, 585–596.
2 G. S. Gould, J. R. Hurst, A. Trofor, J. A. Alison, G. Fox, M. M. Kulkarni, C. E. Wheelock, M. Clarke and R. Kumar, *Respir. Res.*, 2023, **24**, 15.
3 G. C. Gray, E. R. Robie, C. J. Studstill and C. L. Nunn, *Viruses*, 2021, **13**, 637.
4 N. R. Labiris and M. B. Dolovich, *Br. J. Clin. Pharmacol.*, 2003, **56**, 588–599.
5 W. Liang, H. W. Pan, D. Vllasaliu and J. K. W. Lam, *Pharmaceutics*, 2020, **12**, 1025.
6 A. J. Hickey, *Adv. Drug Delivery Rev.*, 2020, **157**, 63–70.
7 S. P. Newman, *Ther. Delivery*, 2017, **8**, 647–661.
8 C. Duret, N. Wauthoz, T. Sebti, F. Vanderbist and K. Amighi, *Int. J. Nanomed.*, 2012, **7**, 5475–5489.
9 W.-H. Lee, C.-Y. Loo, D. Traini and P. M. Young, *Asian J. Pharm. Sci.*, 2015, **10**, 481–489.
10 A. Kermanizadeh, L. G. Powell, V. Stone and P. Møller, *Int. J. Nanomed.*, 2018, **13**, 7575–7605.
11 M. Li, M. Azad, R. Davé and E. Bilgili, *Pharmaceutics*, 2016, **8**, 17.
12 A. Homayouni, M. Sohrabi, M. Amini, J. Varshosaz and A. Nokhodchi, *Mater. Sci. Eng., C*, 2019, **98**, 185–196.
13 R. P. Bakshi, L. M. Tatham, A. C. Savage, A. K. Tripathi, G. Mlambo, M. M. Ippolito, E. Nenortas, S. P. Rannard, A. Owen and T. A. Shapiro, *Nat. Commun.*, 2018, **9**, 315.
14 P. Curley, M. Giardiello, N. J. Liptrott, D. Dickens, D. M. Moss, J. J. Hobson, A. C. Savage, T. O. McDonald, M. Siccardi, S. Rannard and A. Owen, *J. Interdiscip. Nanomed.*, 2017, **2**, 157–169.

© 2025 The Author(s). Published by the Royal Society of Chemistry

Open Access Article. Published on 01 April 2025. Downloaded on 1/18/2026 4:55:59 AM. This article is licensed under a Creative Commons Attribution 3.0 Unported Licence.

15 M. Giardiello, N. J. Liptrott, T. O. McDonald, D. Moss, M. Siccardi, P. Martin, D. Smith, R. Gurjar, S. P. Rannard and A. Owen, *Nat. Commun.*, 2016, **7**, 13184.
16 J. J. Hobson, A. Al-khouja, P. Curley, D. Meyers, C. Flexner, M. Siccardi, A. Owen, C. F. Meyers and S. P. Rannard, *Nat. Commun.*, 2019, **10**, 1413.
17 T. O. McDonald, M. Giardiello, P. Martin, M. Siccardi, N. J. Liptrott, D. Smith, P. Roberts, P. Curley, A. Schipani, S. H. Khoo, J. Long, A. J. Foster, S. P. Rannard and A. Owen, *Adv. Healthcare Mater.*, 2014, **3**, 400–411.
18 H. Zhang, D. Wang, R. Butler, N. L. Campbell, J. Long, B. Tan, D. J. Duncalf, A. J. Foster, A. Hopkinson, D. Taylor, D. Angus, A. I. Cooper and S. P. Rannard, *Nat. Nanotechnol.*, 2008, **3**, 506–511.
19 A. C. Savage, L. M. Tatham, M. Siccardi, T. Scott, M. Vourvahis, A. Clark, S. P. Rannard and A. Owen, *Eur. J. Pharm. Biopharm.*, 2019, **138**, 30–36.
20 T. O. McDonald, L. M. Tatham, F. Y. Southworth, M. Giardiello, P. Martin, N. J. Liptrott, A. Owen and S. P. Rannard, *J. Mater. Chem. B*, 2013, **1**, 4455–4465.
21 T. N. G. Nguyen, V.-T. Tran, W. Duan, P. H. L. Tran and T. T. D. Tran, *Curr. Drug Metab.*, 2017, **18**, 1000–1015.
22 J. Tao, S. F. Chow and Y. Zheng, *Acta Pharm. Sin. B*, 2019, **9**, 4–18.
23 M. O. Jara, Z. N. Warnken and R. O. Williams, *Pharmaceutics*, 2021, **13**, 97.
24 Y. Li, P. Li, Q. He, R. Zhang, Y. Li, N. Kamar, M. P. Peppelenbosch, R. A. de Man, L. Wang and Q. Pan, *Antiviral Res.*, 2022, **197**, 105228.
25 L. Huang, M. Yang, Y. Yuan, X. Li and E. Kuang, *Antiviral Res.*, 2017, **138**, 68–78.
26 R. C. Arend, A. I. Londoño-Joshi, R. S. Samant, Y. Li, M. Conner, B. Hidalgo, R. D. Alvarez, C. N. Landen, J. M. Straughn and D. J. Buchsbaum, *Gynecol. Oncol.*, 2014, **134**, 112–120.
27 J. Liu, X. Chen, T. Ward, Y. Mao, J. Bockhorn, X. Liu, G. Wang, M. Pegram and K. Shen, *Int. J. Biochem. Cell Biol.*, 2016, **71**, 12–23.
28 S. You, R. Li, D. Park, M. Xie, G. L. Sica, Y. Cao, Z.-Q. Xiao and X. Deng, *Mol. Cancer Ther.*, 2014, **13**, 606–616.
29 Q. Fu, X. Jin, Z. Zhang and H. Lv, *Int. J. Pharm.*, 2020, **584**, 119432.
30 E. Barini, A. Miccoli, F. Tinarelli, K. Mulholland, H. Kadri, F. Khanim, L. Stojanovski, K. D. Read, K. Burness, J. J. Blow, Y. Mehellou and M. M. K. Muqit, *ChemBioChem*, 2018, **19**, 425–429.
31 K. Miner, K. Labitzke, B. Liu, P. Wang, K. Henckels, K. Gaida, R. Elliott, J. J. Chen, L. Liu, A. Leith, E. Trueblood, K. Hensley, X.-Z. Xia, O. Homann, B. Bennett, M. Fiorino, J. Whoriskey, G. Yu, S. Escobar, M. Wong, T. Born, A. Budelsky, M. Comeau, D. Smith, J. Phillips, J. Johnston, J. McGivern, K. Weikl, D. Powers, K. Kunzelmann, D. Mohn, A. Hochheimer and J. Sullivan, *Front. Pharmacol.*, 2019, **10**, 51.
32 D. Tilmanis, C. van Baalen, D. Y. Oh, J.-F. Rossignol and A. C. Hurt, *Antiviral Res.*, 2017, **147**, 142–148.
33 S. S. Kapale and H. K. Chaudhari, *J. Indian Chem. Soc.*, 2021, **98**, 100262.
34 E. C. van Tonder, T. S. P. Maleka, W. Liebenberg, M. Song, D. E. Wurster and M. M. de Villiers, *Int. J. Pharm.*, 2004, **269**, 417–432.
35 B. Devarakonda, R. A. Hill, W. Liebenberg, M. Brits and M. M. de Villiers, *Int. J. Pharm.*, 2005, **304**, 193–209.
36 S. Sood, B. Maddiboyina, P. Rawat, A. K. Garg, A. I. Foudah, A. Alam, H. M. Aldawsari, Y. Riadi, S. Singh and P. Kesharwani, *J. Biomater. Sci., Polym. Ed.*, 2021, **32**, 477–487.
37 S. Singh, A. Weiss, J. Goodman, M. Fisk, S. Kulkarni, I. Lu, J. Gray, R. Smith, M. Sommer and J. Cheriyan, *Br. J. Pharmacol.*, 2022, **179**, 3250–3267.
38 U. Arshad, H. Pertinez, H. Box, L. Tatham, R. K. R. Rajoli, P. Curley, M. Neary, J. Sharp, N. J. Liptrott, A. Valentijn, C. David, S. P. Rannard, P. M. O'Neill, G. Aljayyoussi, S. H. Pennington, S. A. Ward, A. Hill, D. J. Back, S. H. Khoo, P. G. Bray, G. A. Biagini and A. Owen, *Clin. Pharmacol. Ther.*, 2020, **108**, 775–790.
39 H. M. Al-Kuraishy, A. I. Al-Gareeb, E. Elekhnawy and G. E.-S. Batiha, *Mol. Biol. Rep.*, 2022, **49**, 11169–11176.
40 A. Fowotade, F. Bamidele, B. Egbetola, A. F. Fagbamigbe, B. A. Adeagbo, B. O. Adefuye, A. Olagunoye, T. O. Ojo, A. O. Adebiyi, O. I. Olagunju, O. T. Ladipo, A. Akinloye, A. Onayade, O. O. Bolaji, S. Rannard, C. Happi, A. Owen and A. Olagunju, *Front. Med.*, 2022, **9**, 956123.
41 J. Xu, P.-Y. Shi, H. Li and J. Zhou, *ACS Infect. Dis.*, 2020, **6**, 909–915.
42 C.-K. Lin, M.-Y. Bai, T.-M. Hu, Y.-C. Wang, T.-K. Chao, S.-J. Weng, R.-L. Huang, P.-H. Su and H.-C. Lai, *Oncotarget*, 2016, **7**, 8993–9006.
43 L. Sweeney, A. P. McCloskey, G. Higgins, J. M. Ramsey, S.-A. Cryan and R. MacLoughlin, *Respir. Res.*, 2019, **20**, 66.
44 J. S. Patton and P. R. Byron, *Nat. Rev. Drug Discovery*, 2007, **6**, 67–74.
45 G. Costabile, I. d'Angelo, G. Rampioni, R. Bondì, B. Pompili, F. Ascenzioni, E. Mitidieri, R. d'Emmanuele di Villa Bianca, R. Sorrentino, A. Miro, F. Quaglia, F. Imperi, L. Leoni and F. Ungaro, *Mol. Pharm.*, 2015, **12**, 2604–2617.
46 A. D. Brunaugh, H. Seo, Z. Warnken, L. Ding, S. H. Seo and H. D. C. Smyth, *PLoS One*, 2021, **16**, e0246803.
47 A. Gupta, S. L. Tulsankar, R. S. Bhatta and A. Misra, *Mol. Pharm.*, 2017, **14**, 1204–1211.
48 J. J. Hobson, A. C. Savage, A. B. Dwyer, C. Unsworth, J. Massam, U. Arshad, H. Pertinez, H. Box, L. Tatham, R. K. R. Rajoli, M. Neary, J. Sharp, A. Valentijn, C. David, P. Curley, N. J. Liptrott, T. O. McDonald, A. Owen and S. P. Rannard, *Nanoscale*, 2021, **13**, 6410–6416.
49 M. Beck-Broichsitter, M.-C. Knuedeler, N. Oesterheld, W. Seeger and T. Schmehl, *Int. J. Pharm.*, 2014, **459**, 23–29.
50 M. B. McGuckin, J. Wang, R. Ghanma, N. Qin, S. D. Palma, R. F. Donnelly and A. J. Paredes, *J. Controlled Release*, 2022, **345**, 334–353.
51 M. Sakagami, W. Kinoshita, K. Sakon, J. Sato and Y. Makino, *J. Controlled Release*, 2002, **80**, 207–218.
52 G. Pilcer and K. Amighi, *Int. J. Pharm.*, 2010, **392**, 1–19.

© 2025 The Author(s). Published by the Royal Society of Chemistry

Open Access Article. Published on 01 April 2025. Downloaded on 1/18/2026 4:55:59 AM.
This article is licensed under a Creative Commons Attribution 3.0 Unported Licence.

53 M. Karhu, J. Kuikka, T. Kauppinen, K. Bergström and M. Vidgren, *Int. J. Pharm.*, 2000, **196**, 95–103.
54 D. E. Walton and C. J. Mumford, *Chem. Eng. Res. Des.*, 1999, **77**, 442–460.
55 G. Bertrand, C. Filiatre, H. Mahdjoub, A. Foissy and C. Coddet, *J. Eur. Ceram. Soc.*, 2003, **23**, 263–271.
56 Y. Dong, W. K. Ng, S. Shen, S. Kim and R. B. H. Tan, *Int. J. Pharm.*, 2009, **375**, 84–88.
57 P. Barski, M. Surdacki, A. Saj, A. Wróblewska, M. Ornat, A. Pawelak, D. Pompa, J. Jurgiel, V. Ermisch, A. Hirnle, I. Pirogowicz, I. Stanisławska, M. Łyp and M. Pokorski, *Physiol. Res.*, 2020, **69**, S131–S137.
58 H.-L. Lin, C.-S. Chen, J. B. Fink, G.-H. Lee, C.-W. Huang, J.-C. Chen and Z. Y. Chiang, *Pharmaceutics*, 2020, **12**, 971.
59 A. Ari and J. B. Fink, *ERJ Open Res.*, 2021, **7**, 00027-2021.
60 P. J. Naughton, M. Joyce, M. Mac Giolla Eain, A. O'Sullivan and R. MacLoughlin, *Pharmaceutics*, 2021, **13**, 1574.
61 L. A. Dailey, T. Schmehl, T. Gessler, M. Wittmar, F. Grimminger, W. Seeger and T. Kissel, *J. Controlled Release*, 2003, **86**, 131–144.
62 A. Farhat, Y. Holloway, T. Jones, S. Taylor, S. Britland and D. Eagland, *J. Pharm. Pharmacol.*, 2009, **61**, A43–A44.
63 M. Shirley, *Drugs*, 2019, **79**, 555–562.
64 V. A. Marple, D. L. Roberts, F. J. Romay, N. C. Miller, K. G. Truman, M. Van Oort, B. Olsson, M. J. Holroyd, J. P. Mitchell and D. Hochrainer, *J. Aerosol Med.*, 2003, **16**, 283–299.
65 ISO 27427:2023(en), Anaesthetic and respiratory equipment—Nebulizing systems and components, **https://www.iso.org/obp/ui/#iso:std:iso:27427:ed-4:v1:en**, (accessed October 3, 2023).
66 A. Hibbitts, A. M. O'Mahony, E. Forde, L. Nolan, J. Ogier, S. Desgranges, R. Darcy, R. MacLoughlin, C. M. O'Driscoll and S. A. Cryan, *J. Aerosol Med. Pulm. Drug Delivery*, 2014, **27**, 466–477.
67 S. P. Newman, *J. Aerosol Med. Pulm. Drug Delivery*, 2022, **35**, 2–10.
68 A. Z. Bahlool, S. Fattah, A. O'Sullivan, B. Cavanagh, R. MacLoughlin, J. Keane, M. P. O'Sullivan and S.-A. Cryan, *Pharmaceutics*, 2022, **14**, 1745.
69 C. Darquenne, *J. Aerosol Med. Pulm. Drug Delivery*, 2020, **33**, 181–185.
70 CDC, COVID-19 and Your Health, **https://www.cdc.gov/coronavirus/2019-ncov/symptoms-testing/symptoms.html**, (accessed October 5, 2023).
71 G. Bennett, M. Joyce, E. F. Fernández and R. MacLoughlin, *Intensive Care Med. Exp.*, 2019, **7**, 20.
72 H. M. Park, K. H. Chang, S.-H. Moon, B. J. Park, S. K. Yoo and K. C. Nam, *Biomed. Eng. Online*, 2021, **20**, 59.

© 2025 The Author(s). Published by the Royal Society of Chemistry